

GENERIC SPECTRUM AND IONIZATION EFFICIENCY OF A HEAVY INITIAL MASS FUNCTION FOR THE FIRST STARS

VOLKER BROMM¹

Department of Astronomy, Yale University, New Haven, CT 06520-8101; volker@ast.cam.ac.uk

ROLF P. KUDRITZKI

Institute for Astronomy, University of Hawaii, 2680 Woodlawn Drive, Honolulu, HI 96822; kud@ifa.hawaii.edu

AND

ABRAHAM LOEB

Astronomy Department, Harvard University, 60 Garden Street, Cambridge, MA 02138;
 aloeb@cfa.harvard.edu

Draft version October 28, 2018

ABSTRACT

We calculate the generic spectral signature of an early population of massive stars at high redshifts. For metal-free stars with mass above $300M_{\odot}$, we find that the combined spectral luminosity per unit stellar mass is almost independent of the mass distribution of these stars. To zeroth order, the generic spectrum resembles a black-body with an effective temperature of $\sim 10^5$ K, making these stars highly efficient at ionizing hydrogen and helium. The production rate of ionizing radiation per stellar mass by stars more massive than $\sim 300M_{\odot}$ is larger by ~ 1 order of magnitude for hydrogen and He I, and by ~ 2 orders of magnitude for He II, than the emission from a standard initial mass function. This would result in unusually strong hydrogen and helium recombination lines from the surrounding interstellar medium. It could also alleviate the current difficulty of ionizing the intergalactic medium at $z \gtrsim 6$ with the cosmic star formation rate inferred at somewhat lower redshifts.

Subject headings: cosmology: theory — early universe — stars: formation — stars: spectra — intergalactic medium

1. INTRODUCTION

One of the most important challenges in modern cosmology is to understand when and how the cosmic “dark ages” ended (Loeb 1998, 1999; Rees 1999). The absence of a Gunn-Peterson trough in the spectra of high-redshift quasars implies that the universe was reionized at a redshift $z > 5.8$ (Fan et al. 2000). An early, pregalactic generation of stars (the so-called Population III) has long been suspected to control this process (e.g., Carr, Bond, & Arnett 1984; Couchman & Rees 1986; Haiman & Loeb 1997). The feedback of the first generation of stars on the ionization history of the intergalactic medium (IGM) depends crucially on their initial mass function (IMF). Recent numerical simulations presented evidence that the primordial IMF might have favored massive stars with a mass $\gtrsim 10^2 M_{\odot}$ (Bromm, Coppi, & Larson 1999, 2001; Abel, Bryan, & Norman 2000). This prediction relies on the existence of a characteristic scale for the density and temperature of the primordial gas, and consequently of a characteristic Jeans mass of $M_J \sim 10^3 M_{\odot}$ (see also Larson 1998). At present, it is not known with any certainty, what fraction of a Jeans-unstable clump of gas will eventually be incorporated into the resulting star. This is due to the complicated physics of the protostellar feedback on a dust-free envelope, and the accretion from it.

Here we adopt the view that the simulated clump masses are indicative of the final stellar masses, and explore the implications. Recent observations of the formation process of present-day stars seem to support this view. Motte,

André, & Neri (1998) have mapped the nearby ρ Ophiuchi star forming cloud in the 1.3 mm dust continuum. Their study identifies a number of dense, gravitationally-bound clumps with masses close to stellar values, which appear to lack the emission from embedded stellar sources. These starless clumps, therefore, might be the direct progenitors of individual stars.

Ultimately, the question of how massive the first stars were, has to be answered by observations. It is therefore important to ask whether future observatories, such as the *Next Generation Space Telescope* (NGST), could place any constraints on the primordial IMF. To address this question, we have constructed models for the interior structure, and the emerging spectra of massive Population III stars. Since metal-free stars have systematically higher effective temperatures ($T_{eff} \sim 10^5$ K for $M > 100M_{\odot}$), they are very efficient at producing photons capable of ionizing hydrogen and helium. The reionization of the intergalactic helium has traditionally been attributed to a population of quasars. A generation of very massive Population III stars would provide an important alternative channel, operating at redshifts higher than what is typically assumed for quasars.

Recently, Tumlinson & Shull (2000) have discussed the case of metal-free stars with a normal (Salpeter-like) IMF, up to masses of $90M_{\odot}$ (see also Ciardi et al. (2000b) for the effect of introducing a lower mass cutoff at $M_c = 5M_{\odot}$). It is important, however, to extend this mass range into the regime of very massive stars with $M > 100M_{\odot}$, since

¹Present address: Institute of Astronomy, University of Cambridge, Madingley Road, Cambridge CB3 0HA, UK

both the nature of the feedback on the IGM, as well as the spectral characteristics, change in a significant way for this regime.

In §2, we describe our models for the stellar interior and for the spectrum. In §3 and §4 we address the ionization efficiency and discuss the observational signatures, respectively. Finally, §5 summarizes the implications of our results.

2. STELLAR MODELS

2.1. *Stellar Structure*

We construct models for static, metal-free stars in complete (i.e., dynamical and thermal) equilibrium by solving the time-independent equations of stellar structure (e.g., Schwarzschild 1958; Kippenhahn & Weigert 1990). The integration is performed in the standard way by fitting solutions for the core and envelope at a suitably chosen intermediate point, and the considered mass range is: $100 \leq M/M_\odot \leq 1000$. Stars in this mass range have traditionally been termed Very Massive Objects, or VMOs (Bond, Arnett, & Carr 1984). For such a massive star with the concomitant high interior temperatures, the only effective source of opacity is electron scattering, given by $\kappa = 0.2(1 + X) \text{ cm}^2 \text{ g}^{-1}$, where $X \simeq 0.76$ is the mass fraction in hydrogen. Other sources of opacity are not included in our calculations.

In the absence of metals, and in particular of the catalysts necessary for the operation of the CNO cycle, nuclear burning proceeds in a non-standard way. At first, hydrogen burning can only occur via the inefficient *pp* chain. To provide the necessary luminosity, the star has to reach very high central temperatures ($T_c \simeq 10^{8.1} \text{ K}$). These temperatures are high enough for the simultaneous occurrence of helium burning via the triple- α process. After a brief initial period of triple- α burning, a trace amount of heavy elements has been formed. Subsequently, the star follows the CNO cycle. In constructing our main-sequence models, we therefore assume a level of pre-enrichment with metals, amounting to a mass fraction of $Z = 10^{-9}$. The resulting models consist of a convective core, containing 90–100% of the mass, and a thin radiative envelope. Due to the high mass and temperature, the stars are dominated by radiation pressure, and have luminosities close to the Eddington limit: $L \simeq L_{\text{EDD}} = 1.25 \times 10^{38} \text{ erg s}^{-1} (M/M_\odot)$.

In this work, we do not include the evolution of the stars away from the main sequence, which crucially depends on the poorly understood mass-loss mechanism. While this is clearly an idealization, it is justified by the fact that the stars spend a major fraction of their total lifetime, estimated to be $\tau \simeq 0.007 M c^2 / L_{\text{EDD}} \sim 3 \times 10^6 \text{ yr}$, near the location of the main-sequence.

In Figure 1, we show the resulting sequence of models for Population III stars, and compare to the corresponding Population I sequence (calculated with $Z = 0.02$). Our results agree well with those of El Eid, Fricke, & Ober (1983) in the mass range $100 < M/M_\odot < 500$. It is evident that the respective effective temperatures approach an asymptotic value which is independent of mass, $T_{\text{eff}} \simeq 1.1 \times 10^5 \text{ K}$ for Population III, and $T_{\text{eff}} \simeq 6.5 \times 10^4 \text{ K}$ for Population I. This characteristic behavior of very massive stars derives from the assumptions of hydrostatic equilibrium,

radiation pressure support with a luminosity close to the Eddington limit, and the nuclear physics of hydrogen burning. The peculiar behavior of very massive Population III stars has already been discussed by a number of previous authors (see Bond, Arnett, & Carr (1984) and references therein). Bond, Arnett, & Carr (1984), in particular, have pointed out that the effective temperature, $T_{\text{eff}} \sim 10^5 \text{ K}$, is almost independent of mass for $M > 100 M_\odot$. For completeness, we here give a somewhat simplified version of the argument.

The mechanical structure of a massive, radiation-pressure dominated star is approximately given by a polytrope of index $n = 3$ (see Kippenhahn & Weigert 1990). If $w(z)$ is the corresponding solution of the Lane-Emden equation, and $z = (z_3/R)r$ the dimensionless radial coordinate, one can express the density and pressure as $\rho = \rho_c w^3$, and $P = (\pi G R^2 \rho_c^{2/3} / z_3^2) \rho^{4/3}$, respectively. Here, $z_3 = 6.89685$ is the dimensionless radius of the polytrope, $\rho_c = 54.1825(3M/4\pi R^3)$ the central density, and the other symbols have their usual meaning. With the polytropic value for the central pressure, $P_c \simeq 11.1 G M^2 / R^4$, one can estimate the temperature at the center of the star, $T_c = (3P_c/a)^{1/4}$, to be

$$T_c \simeq 8.4 \times 10^7 \text{ K} \left(\frac{M}{100 M_\odot} \right)^{1/2} \left(\frac{R}{10 R_\odot} \right)^{-1}. \quad (1)$$

To further constrain T_c , we follow Fowler & Hoyle (1964), and consider the global energy balance of the star. The average nuclear energy generation rate (in $\text{erg s}^{-1} \text{ g}^{-1}$) is $\bar{\epsilon} = L/M = \int_0^M \epsilon dm$, and we assume $\epsilon \simeq \epsilon_{\text{CNO}}$. Writing $\epsilon = \epsilon_c(\rho/\rho_c)(T/T_c)^\nu$, with c denoting central values, one finds

$$\bar{\epsilon} \simeq 162.5 \epsilon_c \left(\frac{1}{z_3^3} \int_0^{z_3} w^{6+\nu} z^2 dz \right). \quad (2)$$

A reasonable fit to the CNO cycle energy generation rate close to $\log T \simeq 8.1$ is given by

$$\epsilon \simeq 1.3 \times 10^{12} Z X \rho \left(\frac{T}{10^8 \text{ K}} \right)^8. \quad (3)$$

This form derives from a linear fit to the exact expression for ϵ_{CNO} (Kippenhahn & Weigert 1990, p. 165), at $\log T \simeq 8.1$. Using $\nu = 8$ in equation (2) gives $\bar{\epsilon} \simeq 0.05 \epsilon_c$. From $L \simeq L_{\text{EDD}} = \bar{\epsilon} M$ follows the desired relation

$$T_c \simeq 1.9 \times 10^8 \text{ K} \left(\frac{Z}{10^{-9}} \right)^{-1/8} \left(\frac{M}{100 M_\odot} \right)^{-1/8} \left(\frac{R}{10 R_\odot} \right)^{3/8}. \quad (4)$$

Combining equations (1) and (4) gives the mass-radius relation for very massive stars

$$M \simeq 370 M_\odot \left(\frac{Z}{10^{-9}} \right)^{-0.2} \left(\frac{R}{10 R_\odot} \right)^{2.2}, \quad (5)$$

from which it can be seen that approximately $M \propto R^2$. Finally, the effective temperature can be estimated from $L \simeq L_{\text{EDD}} = 4\pi R^2 \sigma T_{\text{eff}}^4$. Using equation (5) to eliminate the radius, we find

$$T_{\text{eff}} \simeq 1.1 \times 10^5 \text{ K} \left(\frac{Z}{10^{-9}} \right)^{-0.05} \left(\frac{M}{100 M_\odot} \right)^{0.025}. \quad (6)$$

This analytical estimate for T_{eff} , and the very weak dependence on mass, are in good agreement with the numerical results in Figure 1.

2.2. Emergent Spectrum

Having determined the basic stellar parameters, we now construct model atmospheres and emergent spectra. The extreme luminosities very close to the Eddington limit and the very high effective temperatures require the sophisticated effort of using NLTE unified model atmospheres with spherical extension and stellar winds, as originally introduced by Gabler et al. (1989). This new type of model atmospheres provides a smooth transition from the subsonic, quasi-hydrostatic photosphere to the supersonic, radiation-driven stellar wind, and allows the simultaneous treatment of spectral features formed deep in the photosphere (such as optical continua and line wings) and those arising from the outer layers, where the influence of winds becomes significant (such as strong absorption edges, far infra-red continua and line cores). A detailed discussion is given by Kudritzki (1998).

For our work, we use the new unified model code originally developed by Santolaya-Rey, Puls, & Herrero (1997), and further improved by J. Puls (private communication). Bound-bound, bound-free and free-free absorption by hydrogen and helium, as well as Thomson scattering are included as opacity sources. A value of 0.1 has been adopted for the number ratio of helium to hydrogen. Changing this ratio towards slightly smaller values closer to estimates for the primordial helium abundance would not lead to a significant modification of the calculated spectra.

The atmospheric models are fully specified by the effective temperature, the gravity and the stellar radius (all taken at the Rosseland optical depth $\tau_{ross} = 2/3$) together with the mass-loss rate \dot{M} , the terminal velocity v_∞ , and the parameter β which describes the radial slope of the velocity field via

$$v(r) = v_\infty(1 - b/r)^\beta \quad . \quad (7)$$

The constant b is chosen to guarantee a smooth transition into the hydrostatic stratification at a prespecified outflow velocity smaller than the isothermal sound speed (normally $0.1 c_s$). Velocity fields of this form are predicted by the theory of radiation driven winds (e.g., Castor, Abbott, & Klein 1975; Pauldrach, Puls, & Kudritzki 1986) and usually lead to an excellent fit to observed stellar wind lines based on radiative transfer and model atmosphere calculations (see Kudritzki & Puls 2000).

At zero metallicity, we expect stellar winds to be of only minor importance. However, a radiatively driven wind might still arise due to the opacity in the He II resonance lines, in combination with the contribution from bound-free and free-free absorption. No wind models have been constructed so far for this extreme case of zero metallicity. Kudritzki (2000) has developed a new algorithm, which allows to deal with line driven winds at very low metallicity down to 10^{-4} of the solar value. As a rough extrapolation from his results we adopt $\dot{M} = 10^{-10} M_\odot \text{ yr}^{-1}$, $v_\infty = 1900 \text{ km s}^{-1}$ and $\beta = 1$. This choice of stellar wind parameters results in an almost hydrostatic, but still spherically extended density structure. From a number of additional test calculations carried out with different wind parameters we note that the resulting emergent spectra show only

a very small parameter dependence as long as the winds are weak. For instance, enhancing the mass-loss rate to a value of $\dot{M} = 10^{-8} M_\odot$ has little influence on the energy distribution and line profiles.

In Figure 2, we present the resulting spectra for different masses. Shown is the specific flux, F_ν , at the surface of the star. At these high effective temperatures, there is still a rich spectrum of He II and H lines in the EUV, UV, optical, and IR. Some of these lines show emission features as a result of an overpopulation of their upper levels due to NLTE effects. The He II resonance lines have emission wings and central absorption cores, whereas some of the He II Pickering lines have a central emission peak on top of absorption wings. Such types of line profiles reflect the stratification of the ratio of the NLTE departure coefficients of the upper to the lower line level and are common for very hot stars. A first interpretation of the underlying physics has been given in the pioneering paper by Auer & Mihalas (1972). Strikingly, the He II absorption edge at 228 \AA is very weak or turns into emission for higher masses. This is again a distinct NLTE effect which has been discussed in detail by Husfeld et al. (1984) and Gabler et al. (1989, 1992).

For $M > 300 M_\odot$, the spectra become increasingly similar. This similarity is even more evident when the resulting specific luminosity, $L_\nu = 4\pi R^2 F_\nu$, is plotted per unit stellar mass, as shown in Figure 3. Stars with luminosities close to the Eddington limit, $L_\nu \propto L_{EDD} \propto M$, approach a universal value for their flux per unit mass. The prediction that the total spectral luminosity depends only on the total mass of stars but is *independent of the initial mass function*, is a unique feature of a population of very massive stars. In §4, we explore the observational consequences of this result, but discuss first the production of ionizing photons from these stars.

3. FEEDBACK EFFECTS

The spectrum for a population of very massive, zero-metal stars deviates most strongly from the case with a Salpeter IMF at short wavelengths, near the peak of the corresponding black body at $\lambda_{em} \simeq 250 \text{ \AA}$. An important difference is therefore expected in the rate of producing ionizing photons. To quantify this effect for the species H I, He I, and He II, we calculate the number of ionizing photons per unit stellar mass according to

$$\dot{N}_{ion} = \frac{1}{M} \int_{\nu_{th}}^{\infty} \frac{L_\nu d\nu}{h\nu} \quad , \quad (8)$$

where ν_{th} is the respective threshold for ionization. We here make the somewhat idealized assumption that *all* Population III stars were more massive than $300 M_\odot$. Therefore, as demonstrated in the previous section, their spectra, when scaled to stellar mass, have a generic form which is almost independent of mass. Specifically, we take the luminosity per unit mass, L_ν/M , for a $1000 M_\odot$ star, as given by the dot-dashed line in Fig. 3, to be representative for the generic form, and use it in evaluating the integral in equation (8). The resulting production rates are presented in Table 1. Comparing these rates to the corresponding ones for a Salpeter IMF, as given by Tumlinson & Shull (2000), we find an enhancement in the number of ionizing

photons by a factor of 10 – 20 for H I and He I, and by a factor of ~ 75 for He II. We have verified that using L_ν/M for the $300M_\odot$ case (dotted line in Fig. 3) results in ionization efficiencies that are at most a factor of two smaller: 1.2×10^{48} photons $\text{s}^{-1} M_\odot^{-1}$ for the ionization of H I, 8.6×10^{47} photons $\text{s}^{-1} M_\odot^{-1}$ for He I, and 2.0×10^{47} photons $\text{s}^{-1} M_\odot^{-1}$ for He II. By comparing to Table 1, one can see that our choice of the $1000M_\odot$ spectrum as being representative for the mass range $1000M_\odot > M > 300M_\odot$ is well justified.

To illustrate the implications of this result, consider the following zeroth-order estimate for the fraction of baryons that has to be incorporated into stars, f_* , in order to reionize the respective species. Assuming that η ionizing photons are needed per atom ($\eta > 1$ to account for the effect of recombinations), we find for hydrogen

$$f_*(\text{H I}) \simeq \frac{\eta X}{m_{\text{H}} \tau_{\text{MS}} \dot{N}_{\text{ion}}(\text{H I})} \simeq 10^{-4} \eta_{10} \quad , \quad (9)$$

where $\eta_{10} = (\eta/10)$, and $\tau_{\text{MS}} \simeq 2 \times 10^6$ yr is the approximate main-sequence lifetime of a very massive star. For helium, one has $f_*(\text{He I}) \simeq 10^{-5} \eta_{10}$ and $f_*(\text{He II}) \simeq 4 \times 10^{-5} \eta_{10}$. The corresponding fractions for a Salpeter IMF are $f_* \sim 10^{-3} \eta_{10}$.

Consequently, if the first stars are indeed characterized by a heavy IMF, the intriguing possibility arises that the rare star forming clouds, which originate from the high- σ peaks in the primordial density field, might have played an important role in the reionization of both hydrogen and helium at high redshifts. Furthermore, helium might have even been reionized before hydrogen. Such a sequence of events would be in marked contrast to the standard scenarios of reionization (e.g., Gnedin & Ostriker 1997; Haiman & Loeb 1997; Gnedin 1998; Ciardi et al. 2000a; Haiman, Abel, & Rees 2000; Miralda-Escudé, Haehnelt, & Rees 2000). Recently, Madau, Haardt, & Rees (1999) have pointed out that the known populations of quasars and star-forming galaxies are not sufficient to account for the required number of ionizing photons at redshifts $z \sim 5$. An early generation of very massive stars could alleviate this problem, and contribute a significant part of this unexplained deficit.

4. OBSERVATIONAL SIGNATURE

4.1. Stellar Spectrum

Since the first clusters of stars form prior to the epoch of reionization, they are embedded within a neutral IGM. Consequently, the observed flux shortward of the Ly α resonance wavelength, $\lambda_\alpha = 1216 \text{ \AA}$, will be suppressed by the neutral IGM before reionization (Gunn & Peterson 1965) and by the Ly α forest after reionization. The suppression will be complete (due to the neutral IGM) for observed wavelengths between $(1 + z_{\text{reion}})\lambda_c$ and $(1 + z_s)\lambda_\alpha$ and partial (due to the Ly α forest) at shorter wavelengths (Haiman & Loeb 1999). Here, $\lambda_c = 912 \text{ \AA}$ is the Lyman-limit wavelength, z_s is the source redshift, and z_{reion} is the reionization redshift. The sharp trough of the observed flux at $(1 + z_s)\lambda_\alpha$ can be used to unambiguously determine the redshift of the source, even in the absence of strong spectral lines. To predict the observed spectrum at wavelengths longer than λ_α , we consider $L(\nu_{em})$,

the monochromatic luminosity per unit stellar mass at the emitted frequency ν_{em} . We again make the assumption that the spectrum for a star of $1000M_\odot$ is representative for the mass range $M > 300M_\odot$. With the flux at the surface of the $1000M_\odot$ star being $F(\nu_{em})$, as shown in Figure 2, one has $L(\nu_{em}) = 4\pi R^2 F(\nu_{em})$, where $R \simeq 13.7R_\odot$ is the stellar radius. The observed flux, unattenuated by the neutral IGM, at a frequency $\nu_{obs} = \nu_{em}/(1 + z_s)$ is

$$f(\nu_{obs}) = \frac{L(\nu_{em})}{4\pi r^2(1 + z_s)} \quad , \quad (10)$$

where

$$r = \frac{c}{H_0} \int_0^{z_s} \frac{dz}{\sqrt{\Omega_m(1+z)^3 + \Omega_\Lambda}} \quad . \quad (11)$$

In Figure 4, we show the predicted spectrum for a cluster at $z_s = 10$, assuming a flat universe with $\Omega_\Lambda = 1 - \Omega_m = 0.7$ and a Hubble constant of $H_0 = 65 \text{ km s}^{-1} \text{ Mpc}^{-1}$. We have taken into account the red damping wing of the Gunn-Peterson trough, using the analytical expression given by Miralda-Escudé (1998). In evaluating the optical depth in the vicinity of the Ly α resonance, we assume $z_{\text{reion}} = 7$ and $\Omega_b h = 0.03$, corresponding to a Gunn-Peterson optical depth of $\tau_0(z_s) = 7.4 \times 10^5$. We find that the resulting line shape is not very sensitive to the choice of z_{reion} .

The peak flux is conveniently located in the spectral range between $1 - 5 \mu\text{m}$, where NGST is expected to reach a photometric sensitivity of $\sim 0.1 - 1 \text{ nJy}$. We plot the flux per $10^6 M_\odot$, but it is straightforward to adjust the spectrum to other cases due to the linear scaling with total stellar mass. The composite spectrum of a Salpeter IMF with stellar masses in the range $0.1 \lesssim M/M_\odot \lesssim 100$, has been worked out by Tumlinson & Shull (2000), and is also shown in Figure 4, normalized to the same total stellar mass. In comparing the two spectra, it is evident that the observed flux at any given wavelength is a factor of 5 – 10 larger for the case calculated with a heavy IMF. The difference in absolute flux, however, will not allow to discriminate between the two IMFs, since the total stellar mass of the observed system is not known a priori. One instead has to rely on the difference in colors.

For this purpose, we define the ratios F_{12}/F_{23} and F_{23}/F_{45} , where F_{12} , F_{23} , and F_{45} are the integrated fluxes between $1 - 2 \mu\text{m}$, $2 - 3 \mu\text{m}$, and $4 - 5 \mu\text{m}$, respectively. The two colors can then be expressed as a difference in magnitude

$$\Delta m_A = -2.5 \log \frac{F_{12}}{F_{23}} \quad , \quad (12)$$

and

$$\Delta m_B = -2.5 \log \frac{F_{23}}{F_{45}} \quad . \quad (13)$$

Using the spectra in Figure 4, we find these ratios to be $F_{12}/F_{23} \simeq 2.7$ and $F_{23}/F_{45} \simeq 9.3$ in the case of a heavy IMF, and $F_{12}/F_{23} \simeq 2.5$ and $F_{23}/F_{45} \simeq 7.3$ in the case of a Salpeter IMF. In terms of magnitudes, one has

$$\Delta m_A \simeq \begin{cases} -1.1 & \text{for a heavy IMF} \\ -1.0 & \text{for a Salpeter IMF} \end{cases} \quad ,$$

and

$$\Delta m_B \simeq \begin{cases} -2.4 & \text{for a heavy IMF} \\ -2.1 & \text{for a Salpeter IMF} \end{cases} \quad .$$

Hence, the observed spectrum in the case of a heavy IMF is significantly bluer. Reddening by dust is expected to be weak for the first star clusters (and is already small in some known high-redshift galaxies, see Kudritzki et al. 2000). Moreover, the two colors differentiate between the IMFs in a way that is not degenerate with conventional dust. To see this, we ask: Can the presence of dust in the cluster with a heavy IMF cause the two colors to simultaneously agree with those predicted in the Salpeter case? Applying the average extinction curve for the interstellar medium of the Milky Way (e.g., Savage & Mathis 1979), we adjust the amount of dust present in the cluster such that color A is reddened to agree with the prediction for the Salpeter IMF. The corresponding change in color B results in $\Delta m_B \simeq -1.5$, compared to $\Delta m_B \simeq -2.1$ for the Salpeter IMF. Unless one invokes rather contrived properties for the dust, the photometric signature of a heavy IMF therefore cannot masquerade as the one expected from a Salpeter IMF. By measuring these colors, NGST might thus be able to either confirm or exclude the dominance of very massive stars in the early universe.

4.2. Strong Emission of Recombination Lines

The hard UV emission from a star cluster with a heavy IMF is likely to be reprocessed by the surrounding interstellar medium and produce very strong recombination lines of hydrogen and helium. With \dot{N}_{ion} as derived in §3, the emitted luminosity L_{line}^{em} per unit stellar mass in a particular recombination line can be estimated as follows

$$L_{line}^{em} = p_{line}^{em} h\nu \dot{N}_{ion} (1 - p_{cont}^{esc}) p_{line}^{esc} \quad , \quad (14)$$

where p_{line}^{em} is the probability that a recombination would lead to the emission of a photon in the corresponding line, ν is the frequency of the line and p_{cont}^{esc} and p_{line}^{esc} are the escape probabilities for the ionizing photons and the line photons, respectively. It is natural to assume that the stellar cluster is surrounded by an ionization bounded H II region, and hence p_{cont}^{esc} is close to zero (Wood & Loeb 2000; Ricotti & Shull 2000). In addition, p_{line}^{esc} is likely to be close to unity in the H II region, due to the lack of dust in the ambient metal-free gas. Although the emitted line photons may be scattered by neutral gas, they will diffuse out to the observer and eventually survive if the gas is dust free. Thus, for simplicity, we adopt a value of unity for p_{line}^{esc} .

To be concrete, let us consider case B recombination which yields p_{line}^{em} of about 0.65 and 0.47 for the Ly α and He II 1640 Å lines, respectively. In arriving at these numbers, we assume an electron temperature of $\sim 3 \times 10^4$ K, and an electron density of $\sim 10^2 - 10^3 \text{ cm}^{-3}$ inside the H II region (see Storey & Hummer 1995). With \dot{N}_{ion} from Table 1, we then obtain $L_{line}^{em} = 1.7 \times 10^{37}$ and $2.2 \times 10^{36} \text{ erg s}^{-1} M_{\odot}^{-1}$ for the recombination luminosity of Ly α and He II 1640 Å per embedded stellar mass. A cluster of $10^6 M_{\odot}$ in stars would then produce 4.4 and $0.6 \times 10^9 L_{\odot}$ in the Ly α and He II 1640 Å lines. Similarly high luminosities would be produced in other recombination lines at longer wavelengths, such as He II 4686 Å and H α .

The rest-frame equivalent width of these emission lines measured against the stellar continuum of the embedded

cluster at the line wavelengths is given by

$$W_{\lambda} = \left(\frac{L_{line}^{em}}{L_{\lambda}} \right) \quad , \quad (15)$$

where L_{λ} is the spectral luminosity per unit wavelength of the stars at the line resonance. From Figure 3, we obtain a spectral luminosity per unit frequency $L_{\nu} = 2.7 \times 10^{21}$ and $1.8 \times 10^{21} \text{ erg s}^{-1} \text{ Hz}^{-1} M_{\odot}^{-1}$ at the corresponding wavelengths. Converting to L_{λ} , we obtain rest-frame equivalent widths of $W_{\lambda} = 3100 \text{ Å}$ and 1100 Å for Ly α and He II 1640 Å, respectively. These extreme emission equivalent widths are more than an order of magnitude larger than the expectation for a normal cluster of hot stars with the same total mass and a Salpeter IMF under the same assumptions concerning the escape probabilities and recombination (e.g., Kudritzki et al. 2000). The equivalent widths are, of course, larger by a factor of $(1+z_s)$ in the observer frame. Extremely strong recombination lines, such as Ly α and He II 1640 Å, are therefore expected to be an additional spectral signature that is unique to very massive stars in the early universe. Tumlinson & Shull (2000) have discussed the possible observational role of the He II 1640 Å line in the context of a standard Salpeter IMF.

The He II 1640 Å line would reach the observer unaffected by the intervening IGM, since its wavelength is longer than that of the Ly α transition which dominates the IGM opacity. However, the Ly α line emitted by the source would be resonantly scattered by the intergalactic H I. At redshifts lower than the reionization redshift, most of the IGM is ionized and only the blue wing of the line would be suppressed by the Ly α forest. But if the star cluster lies beyond the reionization redshift, the intervening neutral IGM acts as fog and obscures the view of the source at the Ly α wavelength. The line photons emitted by the source scatter until they eventually redshift out of resonance and escape due to the Hubble expansion of the surrounding intergalactic H I. As a result, the source creates a faint Ly α halo on the sky (Loeb & Rybicki 1999). For a source at $z_s \sim 10$, the halo occupies an angular radius of $\sim 15''$ and corresponds to a line that is broadened and redshifted by $\sim 10^3 \text{ km s}^{-1}$ relative to the source. The scattered photons are also highly polarized (Rybicki & Loeb 1999). A heavy IMF would make the detection of diffuse Ly α halos around the first star clusters more accessible to future telescopes, and would provide an important tool for probing the neutral IGM prior to the epoch of reionization. Observations which focus directly on the bright central source are more straightforward, and should show a strong suppression of the Ly α line by the damping-wing of the “Gunn-Peterson trough”, caused by the IGM scattering (Miralda-Escudé 1998). The very brightest sources might be an exception, in that the H II region they generate in the surrounding IGM might shift the Ly α damping wing and allow a portion of the red wing of the emission line to be observed (Cen & Haiman 2000; Madau & Rees 2000).

5. SUMMARY AND CONCLUSIONS

We have explored the consequences of a possible early generation of very massive, zero-metal stars. These stars are almost fully convective, have luminosities close to the Eddington limit, and effective temperatures, $T_{eff} \sim 10^5 \text{ K}$,

which are almost independent of stellar mass. Using a spherically extended, NLTE stellar atmosphere code, we have subsequently constructed the emerging spectra. If normalized by the mass of the star, the spectrum has a generic form, almost independent of mass for $M \gtrsim 300M_{\odot}$. Based on the photometric colors of the composite spectrum from a cluster of Population III stars, we find that it would be feasible observationally to constrain the primordial IMF with future infrared telescopes such as NGST (Fig. 4).

We also investigated the ionizing photon production from these massive stars. Compared to a population of stars with a normal, Salpeter-like IMF, the rate of producing ionizing photons is enhanced by an order of magnitude for H and He I, and by a factor of ~ 100 for He II. As a result, the interstellar medium of a star cluster with a heavy IMF is likely to generate extremely strong recombination lines, such as $\text{Ly}\alpha$ and He II 1640 Å, with equivalent widths that are larger by at least an order of magnitude compared to a standard IMF.

Very massive Population III stars might have played a significant role in the reionization of the hydrogen and helium in the IGM at high redshifts. The ability to efficiently ionize He II provides an alternative channel for a process which has otherwise to rely on the presence of quasars with their non-thermal spectra. Equally important is the possible contribution of massive stars to the ionizing photon budget at $z \sim 5$, where the known quasars and galaxies

are unable to maintain the IGM in an ionized state as long as the IMF is assumed to have the standard form (Madau et al. 1999).

The massive stars considered in this work are likely to end up as black holes (Fryer, Woosley, & Heger 2000). If γ -ray bursts (GRBs) originate from the collapse of these massive stars, then a heavy IMF will produce a larger abundance of GRBs at high redshifts than previously estimated (Ciardi & Loeb 2000). The bright afterglows of these GRBs would provide an important probe of the IGM at high-redshifts (Lamb & Reichart 2000).

A valuable contribution to the early stages of this work was made by Pierre Demarque, who adapted the Yale stellar structure code to compute models of very massive zero-metallicity stars; although the results reported in this paper were obtained with a more efficient code kindly supplied by Dimitar Sasselov, the models of Pierre Demarque provided an important check on their correctness. The authors wish to thank Joachim Puls for the assistance in using his unified model atmosphere code, and Michael Shull and Jason Tumlinson for making available to us their composite Population III spectrum. We are grateful to Martin Haehnelt and Martin Rees for helpful discussions. VB thanks Paolo Coppi for financial support under NASA grant NAG5-7074, and AL acknowledges support by NASA grant NAG 5-7768 and NSF grant AST-0071019.

REFERENCES

- Abel, T., Bryan, G. L., & Norman, M. L. 2000, ApJ, in press (astro-ph/0002135)
- Auer, L. H., & Mihalas, D. 1972, ApJS, 24, 193
- Bond, J.R., Arnett, W.D., & Carr, B.J. 1984, ApJ, 280, 825
- Bromm, V., Coppi, P. S., & Larson, R. B. 1999, ApJ, 527, L5
- Bromm, V., Coppi, P. S., & Larson, R. B. 2001, ApJ, submitted
- Carr, B.J., Bond, J.R., & Arnett, W.D. 1984, ApJ, 277, 445
- Castor, J. I., Abbott, D. C., & Klein, R. I. 1975, ApJ, 195, 157
- Cen, R. & Haiman, Z. 2000, ApJL, submitted (astro-ph/0006376)
- Ciardi, B., Ferrara, A., Governato, F., & Jenkins, A. 2000a, MNRAS, 314, 611
- Ciardi, B., Ferrara, A., Marri, S., & Raimondo, G. 2000b, MNRAS, submitted (astro-ph/0005181)
- Ciardi, B., & Loeb, A. 2000, ApJ, in press (astro-ph/0002412)
- Couchman, H. M. P., & Rees, M. J. 1986, MNRAS, 221, 53
- El Eid, M. F., Fricke, K. J., & Ober, W. W. 1983, A&A, 119, 54
- Fan, X. et al. 2000, AJ, submitted (astro-ph/0005414)
- Fowler, W. A., & Hoyle, F. 1964, ApJS, 9, 201
- Fryer, C. L., Woosley, S. E., & Heger, A. 2000, ApJ, submitted (astro-ph/0007176)
- Gabler, R., Gabler, A., Kudritzki, R. P., Puls, J., & Pauldrach, A. 1989, A&A, 226, 162
- Gabler, R., Gabler, A., Kudritzki, R. P., Mendez, R.H. 1992, A&A, 265, 656
- Gnedin, N. Y., & Ostriker, J. P. 1997, ApJ, 486, 581
- Gnedin, N. Y. 1998, MNRAS, 294, 407
- Gunn, J. E., & Peterson, B. A. 1965, ApJ, 142, 1633
- Haiman, Z., & Loeb, A. 1997, ApJ, 483, 21
- Haiman, Z., & Loeb, A. 1999, ApJ, 519, 479
- Haiman, Z., Abel, T., & Rees, M. J. 2000, ApJ, 534, 11
- Husfeld, D., Kudritzki, R. P., Simon, K. P., & Clegg, R. E. S. 1984, A&A, 134, 139
- Kippenhahn, R., & Weigert, A. 1990, Stellar Structure and Evolution (Heidelberg: Springer)
- Kudritzki, R. P. 1998, in "Stellar Astrophysics for the Local Group", VIII Canary Islands Winter School of Astrophysics, ed. A. Aparicio, A. Herrero, & F. Sanchez (Cambridge: Cambridge University Press), 149
- Kudritzki, R. P. 2000, in "The First Stars", ESO Astrophysics Symposia, ed. A. Weiss, T. Abel, & V. Hill (Berlin: Springer), 127
- Kudritzki, R. P. et al. 2000, ApJ, 536, 19
- Kudritzki, R. P., & Puls, J., 2000, ARA&A, 38, 613
- Lamb, D. Q., & Reichart, D. E. 2000, ApJ, 536, 1
- Larson, R. B. 1998, MNRAS, 301, 569
- Loeb, A. 1998, in ASP Conf. Ser. 133, Science with the Next Generation Space Telescope, ed. E. Smith & A. Koratkar (San Francisco: ASP), 73
- Loeb, A. 1999, to appear in PASP proc. of the conference on "The Hy-Redshift Universe: Galaxy Formation and Evolution at High Redshift", Berkeley, June 1999, ed. A.J. Bunker & W.J.M. van Breugel (astro-ph/9907187)
- Loeb, A., & Rybicki, G. B. 1999, ApJ, 524, 577
- Madau, P., Haardt, F., & Rees, M. J. 1999, ApJ, 514, 648
- Madau, P., & Rees, M. J. 2000, ApJL, submitted (astro-ph/0006271)
- Miralda-Escudé, J. 1998, ApJ, 501, 15
- Miralda-Escudé, J., Haehnelt, M., & Rees, M. J. 2000 ApJ, 530, 1
- Motte, F., André, P., & Neri, R. 1998, A&A, 336, 150
- Pauldrach, A., Puls, J., & Kudritzki, R. P. 1986, A&A, 164, 86
- Rees, M. J. 1999, in AIP Conf. Proc. 470, After the Dark Ages: When Galaxies were Young (the Universe at $2 < z < 5$), ed. S. S. Holt & E. Smith (Woodbury: AIP), 13
- Ricotti, M., & Shull, J. M. 2000, ApJ, in press (astro-ph/9912006)
- Rybicki, G. B., & Loeb, A. 1999, ApJ 520, L79
- Santolaya-Rey, A. E., Puls, J., & Herrero, A., 1997, A&A, 323, 488
- Savage, B. D., Mathis, J. S., 1979, ARA&A, 17, 73
- Schwarzschild, M. 1958, Structure and Evolution of the Stars (Princeton: Princeton Univ. Press)
- Storey, P. J., & Hummer, D. G., 1995 MNRAS 272, 41
- Tumlinson, J., & Shull, J.M. 2000, ApJ, 528, L65
- Wood, K., & Loeb, A. 2000, ApJ, in press (astro-ph/9911316)

TABLE 1
PRODUCTION OF IONIZING PHOTONS ^a

	E [eV]	\dot{N}_{ion} [photons s ⁻¹ M_{\odot}^{-1}]	Y	f_{\star}/η_{10}
H I	13.6	1.6×10^{48}	~ 16	1×10^{-4}
He I	24.6	1.1×10^{48}	~ 14	1×10^{-5}
He II	54.4	3.8×10^{47}	~ 75	4×10^{-5}

^aThe production rates are calculated for a $1000M_{\odot}$ star. Within a factor of two, these rates apply to all stars with mass above $300M_{\odot}$.

NOTE.— E is the ionization potential, \dot{N}_{ion} is the production rate of ionizing photons per unit stellar mass, Y is the ratio of \dot{N}_{ion} for the cases of a heavy IMF and a Salpeter IMF, and f_{\star} is the required baryon fraction that needs to be converted into stars in order to produce $10\eta_{10}$ ionizing photons per species particle (H I, He I, or He II).

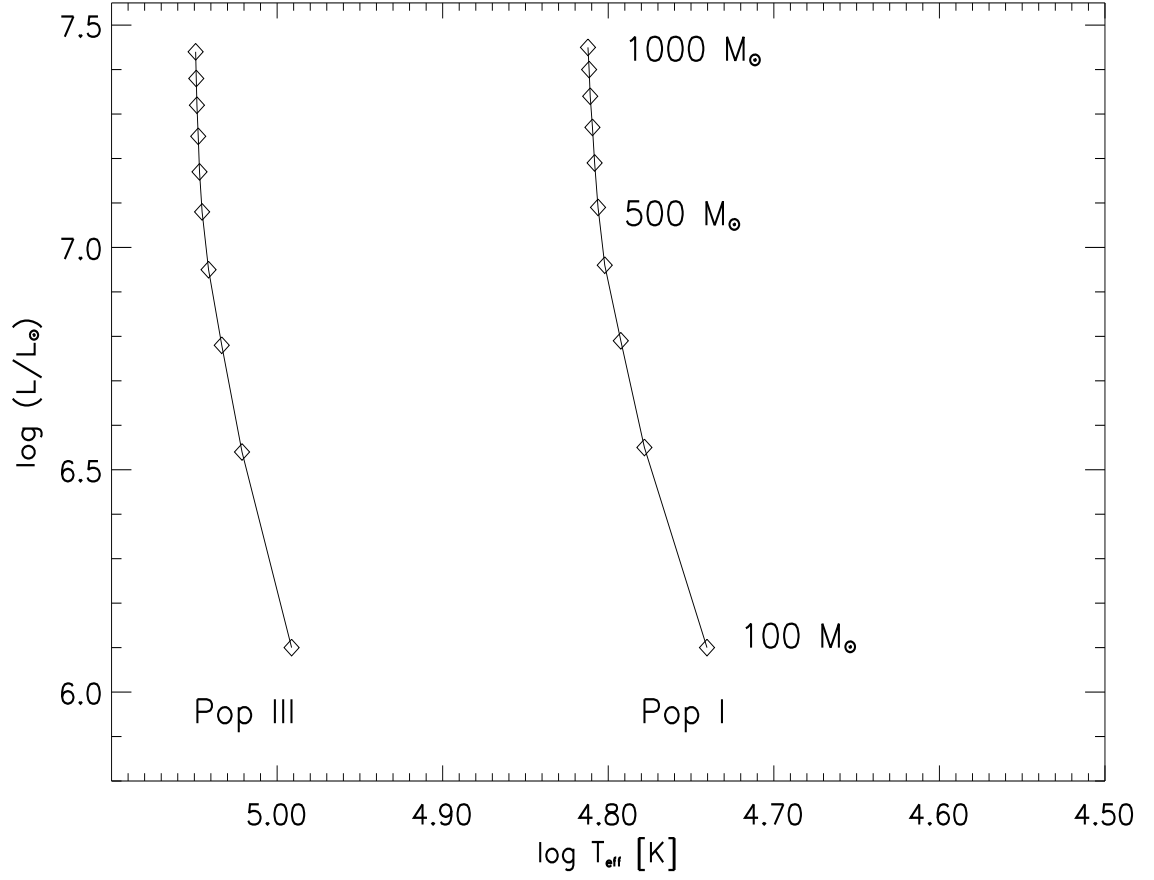


FIG. 1.— Zero-age main sequence of very massive stars. *Left solid line:* Population III zero-age main sequence (ZAMS). *Right solid line:* Population I ZAMS. In each case, stellar luminosity (in L_{\odot}) is plotted vs. effective temperature (in K). *Diamond-shaped symbols:* Stellar masses along the sequence, from $100M_{\odot}$ (bottom) to $1000M_{\odot}$ (top) in increments of $100M_{\odot}$. The Population III ZAMS is systematically shifted to higher effective temperature, with a value of $\sim 10^5$ K which is approximately independent of mass. The luminosities, on the other hand, are almost identical in the two cases.

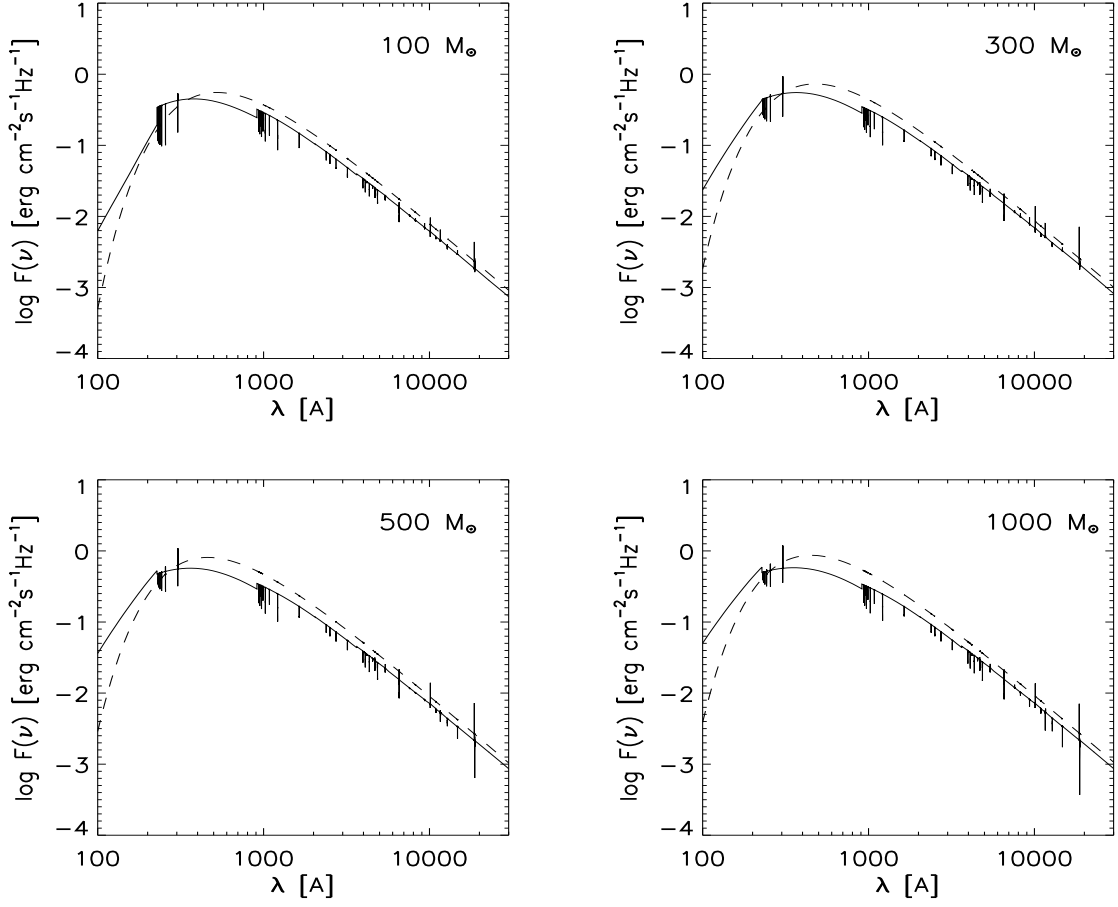


FIG. 2.— Spectra of very massive Population III stars. *Solid lines*: Flux at the surface of the star (in units of $\text{erg s}^{-1} \text{cm}^{-2} \text{Hz}^{-1}$) vs. wavelength (in \AA). *Dashed lines*: Corresponding black-body spectrum, evaluated at the respective effective temperatures. Lines are due to transitions of H and He II in the EUV, UV, optical, and IR bands. The spectra for $M = 100, 300, 500$, and $1000 M_{\odot}$ are remarkably similar, differing only slightly in the strengths of the He II and H I ionization edges at 228 \AA and 912 \AA , respectively.

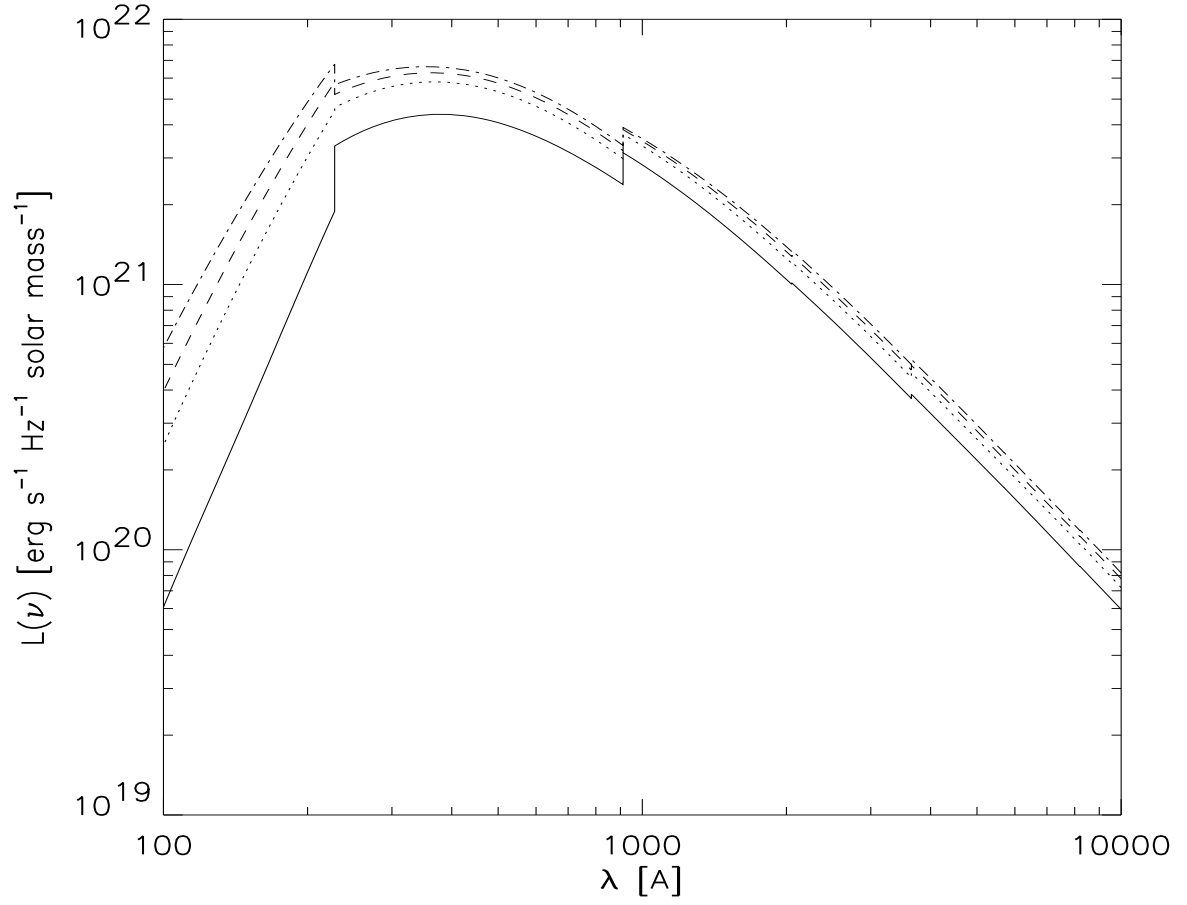


FIG. 3.— The normalized spectral energy distribution in the continuum. Luminosity per unit stellar mass (in $\text{erg s}^{-1} \text{Hz}^{-1} \text{solar mass}^{-1}$) vs. wavelength (in \AA). *Solid line*: $100M_{\odot}$. *Dotted line*: $300M_{\odot}$. *Dashed line*: $500M_{\odot}$. *Dot-dashed line*: $1000M_{\odot}$. When plotted per unit mass, the spectra admit an almost universal form for $M > 300M_{\odot}$.

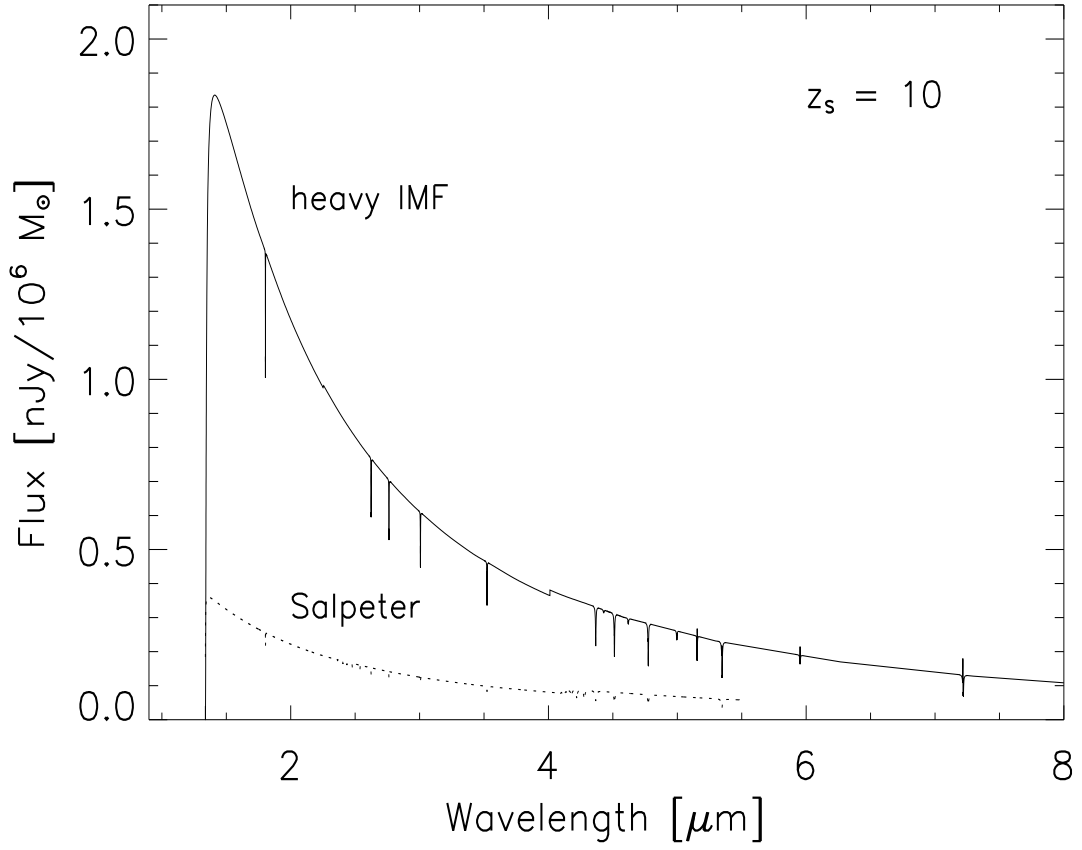


FIG. 4.— The predicted flux from a Population III star cluster at $z_s = 10$. Observed flux (in nJy per $10^6 M_\odot$ of stars) vs. wavelength (in μm). We assume a flat universe with $\Omega_\Lambda = 0.7$, and a Hubble constant of $H_0 = 65 \text{ km s}^{-1} \text{ Mpc}^{-1}$. *Solid line*: The case of a heavy IMF. *Dotted line*: The comparison case of a standard Salpeter IMF, where the composite spectrum is taken from Tumlinson & Shull (2000). The cutoff below $\lambda_{obs} = 1216 \text{ \AA} (1 + z_s) = 1.34 \mu\text{m}$ is due to complete Gunn-Peterson absorption. It can be seen that for the same amount of total stellar mass, the observable flux is larger by an order of magnitude for stars which are distributed according to a heavy IMF.